SOLAR ENGINEERING SOLAR
ENGINEERING MATERIAL SCIENCE

Production and Characteristics of $(ZnSe)_{0.1}(SnSe)_{0.9}$ Films for Use in Thin Film Solar Cells

T. M. Razykov[a], B. A. Ergashev[a], R. T. Yuldoshov[a], A. A. Mavlonov[a], and K. M. Kuchkarov[a], *

[a]Physical-Technical Institute, Academy of Sciences
of the Republic of Uzbekistan, Tashkent, 100084 Uzbekistan
*e-mail: k.kuchkarov@mail.ru

Abstract—$(ZnSe)_x(SnSe)_{1-x}$ films have been produced using chemical molecular beam deposition (CMBD) from an ZnSe and SnSe compound with a stoichiometric composition at a substrate temperature of 500°C. The structural, morphological, and electrophysical properties of $(ZnSe)_{0.1}(SnSe)_{0.9}$ films are studied. The size of film grains is 5–6 μm. The results of X-ray diffraction analysis of specimens have revealed that the films have a crystalline (orthorhombic) structure. The structural parameters of the produced films are presented. The electrical conductivity of the films measured using the Van der Pauw method varies within 15–0.6 Ω cm^{-1}.

INTRODUCTION

Thin film solar cells based on CdTe and Cu(In, Ga)Se$_2$ are among the most suitable for large-scale use due to their basic properties. These cells have an optimal band gap width at room temperature E_g = 1.5 eV for CdTe and 0.9–1.7 eV for Cu(In, Ga)Se$_2$, they cover the entire of infrared and visible spectrum of sunlight, and they have a high absorption coefficient (~10^4–10^5 cm^{-1}), with which incident sunlight is absorbed to a thickness of several microns. This significantly reduces material consumption compared to silicon solar cells.

Table 1 gives the latest advances in the efficiency of thin film solar cells achieved by the various methods and scientific centers. As is seen, the efficiency of film solar cells increases from year to year. The leading companies in this field are First Solar and ZSW, which obtained the highest efficiency values for solar cells based on CdTe and Cu(In, Ga)Se$_2$ in laboratory conditions: 22.1 [1] and 22.3% [2]; in modules, 16.1% [3] and 17% [4], respectively.

Despite the high efficiency of solar cells based on these materials, their further use on a wide-scale basis is limited due to the low content of In, Ga, Te in the Earth's crust; as well, gallium (Ga), which is included in the structural composition, is exorbitantly expensive.

That is why many scientific centers and laboratories are engaged in research to replace these expensive materials with widely available elements, such as Cu$_2$ZnSnS$_4$ (CZTS). The main optical properties of these materials are similar to Cu(In, Ga)Se$_2$. An advantage of these elements is their low cost (natural abundance) and nontoxicity.

As is seen from Table 1, 12.6% efficiency of solar cells based on Cu$_2$ZnSnS$_x$Se$_{4-x}$ of [5] has been achieved by the IBM research center within the past 20 years. However, this efficiency is significantly lower compared to Cu(In,Ga)Se$_2$. According to studies by the researchers [6], the low efficiency is explained by the complexity of the methods for producing and controlling the film composition.

To achieve high efficiency with thin film solar cells, novel structures are being developed and studied: SnSe, CuSb(S$_{1-x}$Se$_x$)$_2$, Cu$_2$(Sn$_{1-x}$Ga$_x$)Se$_3$ (CTGS), and Cu$_2$SnS$_3$. The elements included in the composition of these structures are also low-cost and nontoxic. These new materials are attractive and have the same properties as Cu(In, Ga)Se$_2$, such as a band gap width within the range of 0.87–1.7 eV [7–9]. The first attempt to produce thin film solar cells on their basis yielded an efficiency result of 4–6% [10–13]. At present, researchers are working to increase the efficiency of such solar cells.

Despite the fact that there is no information in the world literature about zinc and tin sulfoselenide (Zn$_x$Sn$_{1-x}$Se$_y$S$_{1-y}$) in the form of thin films, this promising new material is suitable for use in photovoltaics. It

Table 1. Achievements in efficiency of solar cells based on CdS/CdTe, Cu(In,Ga)Se$_2$ and Cu$_2$ZnSnS$_x$Se$_{4-x}$ produced by various methods and companies [16, 17]

Year	Type	CdS and CdTe/ process	Activation process	V_{oc}, mV	I_{sc}, mA/cm^2	FF, %	η, %	Area, cm^2	Group
1993	Glass/SnO$_2$:F/CdS/CdTe	CBD/CSS	Thermal evaporation of CdCl$_2$	843	25.1	74.5	15.8	1.05	USF
2001	Glass /CTO/ZTO/CdS/CdTe	CBD/CSS	Thermal evaporation of CdCl$_2$	845	25.9	75.5	16.5	1.03	NREL
2013	Glass/CTO/ZTO/CdS/CdTe	CBD/CSS	Thermal evaporation of CdCl$_2$	875	28.9	78.0	19.7	1	First Solar
2014	Glass /CTO/ZTO/CdS/CdTe	CBD/CSS	Thermal evaporation of CdCl$_2$	872	29.5	79.5	20.4	1	First Solar
2016	Glass /CTO/ZTO/CdS/CdTe	CBD/CSS	Thermal evaporation of CdCl$_2$	903	30	79.8	22.1	1	First Solar
2014	Glass /Mo/Cu(In,Ga)Se/CdS/ ZTO/ZTO:Al			757	34.8	79.1	20.8	0.5	ZSW
2014	Glass /Mo/Cu(In,Ga)Se/CdS/ ZTO/ZTO:Al			746	36.6	79.3	21.7	0.5	ZSW
2016	Glass /Mo/Cu(In,Ga)Se/CdS/ ZTO/ZTO:Al	Thermal evaporation		741	37.8	80.6	22.6	0.5	ZSW
2008	Glass /Mo/CuZTS/CdS/ ZTO/ITO	Thermal evaporation		661	19.5	65.8	8.4	0.46	IBM
2012	Glass /Mo/CuZTSS/CdS/ ZTO/ITO/CdS/ ZTO/ITOl	Growth from solution		460	34.5	69.8	11.1	0.44	IBM
2013	Glass /Mo/ CuZTSS/CdS/ ZTO/ITO	Growth from solution		513.4	35.2	69.8	12.6	0.44	IBM

PM, printing method; CSS, close-spaced sublimation; CBD, Chemical bath deposition; USF, University of South Florida; NREL, National Renewable Energy Laboratory; ZSW, Zentrum für Sonnenenergie-und Wasserstoff-Forschung (Center of Solar and Hydrogen Energy Researches); IBM (MFA), International Business Machines. CTO, Cd$_2$SnO$_4$; ZTO, ZnO: CuZTS, Cu$_2$ZnSnS$_4$; CuZTSS, Cu$_2$ZnSnS$_{4-x}$Se$_x$.

is formed by widely available and environmentally safe elements with excellent physical properties:

—The band gap width can vary within a wide range (0.9−2.7 eV), which is suitable for the absorbing layer with the optimal band gap width within the range of 1.45 eV. Using this material, a thin film solar cell can be produced with an efficiency of photovoltaic energy conversion of 20−25%.

—The absorption coefficient is within the range of $10^4−10^5$ cm^{-1}. This means that an absorbing layer 0.5−1.0 μm thick is sufficient to produce high-efficiency solar cells.

The mobility of holes within the range 500−1000 cm^2/(V s) is observed in thin SnS and SnSe films [14] and in the thin films ZnSe, which demonstrate hole mobility significantly exceeding 100 cm^2/(V s) [15]. Therefore, the value for the hole mobility of a mixed $Zn_xSn_{1−x}Se_yS_{1−y}$ compound is 100 cm^2/(V s) or more.

Earlier, the authors studied the physical properties of the films CdTe [18], SnSe [19], SbSe [20] and $Zn_xCd_{1−x}S$ [21] produced using the method of chemical molecular beam deposition in the hydrogen flow.

This study investigates the physical properties of the films $(ZnSe)_x(SnSe)_{1−x}$ with the composition $x = 0.1$ and produced at a substrate temperature of 500°C using chemical molecular beam deposition (CMBD).

EXPERIMENTAL

A polycrystalline $(ZnSe)_x(SnSe)_{1−x}$ film was produced according to the method described in [22]. The synthesis of $(ZnSe)_x(SnSe)_{1−x}$ films by the CMBD was carried out as follows. Powders of the SnSe and ZnSe compound with a stoichiometric composition were loaded into each container. Then, the system was brought to the operating conditions and blown with hydrogen to remove atmospheric contaminant gases. Then, the external furnace of the soaking chamber was activated. The heating level was determined by the specified deposition temperatures. When the required heating level of the substrate was achieved, the furnace for individual heating of the SnSe, ZnSe compound was activated and brought to the required evaporation temperature. The temperature evaporation interval to grow the films is within 850−950°C, and the substrate temperature varied within 500−600°C. The gas flow of the hydrogen carrier was ~20 cm^3/min. The duration of the deposition process depended on the required film thickness within the range of 30−60 min. Borosilicate glass was used as the substrate.

The crystalline structure and phase composition of the materials were studied by XRD using a Panalytical Empyrean diffractometer with CuK$_\alpha$ radiation (λ = 1.5418 Å) measurement of 2θ within the range 20°−80° and pitch of 0.01°. The phase composition was analyzed with the Joint Committee on Powder Diffraction Standard (JCPDS) database. Morphological studies were performed on an EVO MA 10 scanning electron microscope (SEM).

Ohmic contacts were applied to the as-deposited films by vacuum deposition for electrical measurements. Silver and silver paste were used as ohmic contacts with the hole conductivity films, and an indium or indium−gallium alloy was used with electron conductivity films. The type of conductivity for the specimen was determined according to the sign of the thermal electromotive force. A film thickness of 1−3 μm was determined on an MII-4 microinterferometer, as well as by precision microweighing on FA 1204C scales (with an accuracy of 0.1 mg). After production of the ohmic contacts, the "dark" characteristics of the film were measured. Analysis of the dark volt-ampere characteristic of the films $(ZnSe)_x(SnSe)_{1−x}$ showed that all specimen were "ohmic"; i.e., they did not detect any rectifications within the range of measured voltages ($U = 0.01−2$ V).

RESULTS AND DISCUSSION

The $(ZnSe)_{0.1}(SnSe)_{0.9}$ films produced at a substrate temperature of 500°C had a smooth surface without cracks or pores and densely covered the substrate surface. The physical properties of the film depending on the deposition conditions are presented below.

Figure 1 shows the X-ray pattern for $(ZnSe)_{0.1}(SnSe)_{0.9}$ films produced at a substrate temperature of 500°C. The main peaks in the X-ray pattern were those corresponding to the (400) and (800) planes (Fig. 1). The total intensity of the peaks of the (400) and (800) planes for the specimens was 90−95% of the total intensity of all peaks of the $(ZnSe)_{0.1}(SnSe)_{0.9}$ films in the X-ray pattern. The peaks corresponding to the (200), (201), (111), (400), 600), (511), (402), (502), (303) and (323) planes, the intensity of which was very low compared to the intensity of the (400) and (800) peaks, were also present in the X-ray patterns of the specimens together with the peaks of the specified planes. As seen from the X-ray pattern, almost all of the observed peaks of the $(ZnSe)_{0.1}(SnSe)_{0.9}$ films correspond to the peaks present in the SnSe phase. According to the XRD analysis results, the films has an orthorhombic structure. The parameters of the crystal lattice for the specimens were calculated by the formula

$$\frac{1}{d^2} = \frac{h^2}{a^2} + \frac{k^2}{b^2} + \frac{l^2}{c^2},$$

where d is the distance between the planes and h,k,l are the Miller indices. The parameters of the lattice constant for the films deposited from ZnSe and SnSe compounds at a substrate temperature of 500°C have the following values: $a = 11.48$ Å, $b = 3.78$ Å, $c = 4.47$ Å. Table 2 gives the structural parameters of the
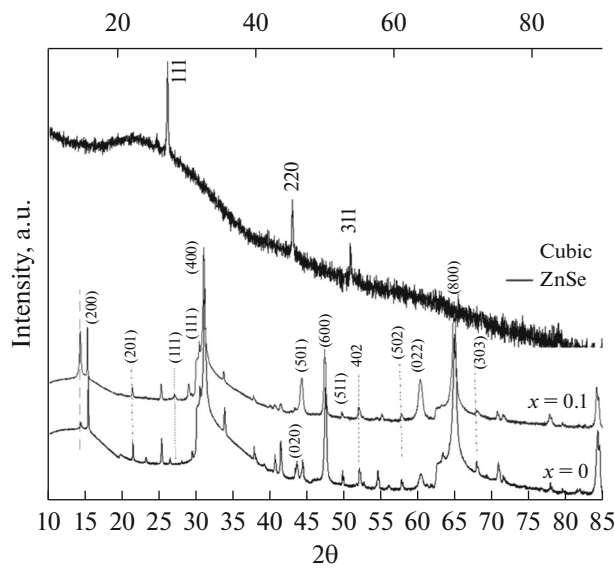
Fig. 1. X-ray patterns of films produced from ZnSe and SnSe compound at substrate temperature of 500°C.

$(ZnSe)_{0.1}(SnSe)_{0.9}$ films: the values of crystal lattice parameters a and b for the $(ZnSe)_{0.1}(SnSe)_{0.9}$ films decrease, and the c value increases as compared to the crystal lattice parameters of the $(ZnSe)_x(SnSe)_{1-x}$ films for $x = 0$. The structural parameters of the $(ZnSe)_x(SnSe)_{1-x}(x = 0)$ films are given in [19]. These changes may occur because with an increase in the molar content of ZnSe in the vapor phase as the

$(ZnSe)_{0.1}(SnSe)_{0.9}$ films are produced, the Sn atoms are replaced by Zn atoms. It is known that the ion radius of zinc (Zn^+ 0.88 Å) is less than the ion radius of tin (Sn^+ 0.93 Å).

Figure 2 shows SEM images for the specimens deposited from the ZnSe and SnSe compound with a stoichiometric composition at a substrate temperature of 500°C.

As is seen from Fig. 2, the shapes of the specimen grains deposited at a temperature of 500°C had a simplified form and the size of the film grains was 5–6 μm. The microstructure of the $(ZnSe)_{0.1}(SnSe)_{0.9}$ films revealed no visible change in the size and shape of grains corresponding to the film having the composition with $x = 0$.

The specific resistance of the films was measured using the Van der Pauw method to study the influence of the ratio of the ZnSe and SnSe molecular beam intensities in the vapor phase on the electrical properties of the $(ZnSe)_x(SnSe)_{1-x}$ films. Thermoelectrical studies showed that all produced films had p-type conductivity. Table 3 gives the obtained results for $(ZnSe)_x(SnSe)_{1-x}$ films with the following compositions $x = 0$; 0.1 (σ, ρ, and type of conductivity).

As seen from Table 3, an increase in the specific resistance (6×10^{-2} Ω cm) of $(ZnSe)_{0.1}(SnSe)_{0.9}$ films was observed compared to ρ (6.2 Ω cm) of SnSe films. The increased specific resistance of $(ZnSe)_{0.1}(SnSe)_{0.9}$ films with increasing the ZnSe content of the wide

Table 2. Structural parameters of $(ZnSe)_{0.1}(SnSe)_{0.9}$ films produced at substrate temperature of 500°C

Films $(ZnSe)_x(SnSe)_{1-x}$ deposited from ZnSe and SnSe composition				
film composition				
x = 0.1				x = 0
crystal lattice parameters, Å	2Θ	(h k l)	d, Å	crystal lattice parameters, Å
a = 11.48 b = 3.78 c = 4.47	15.4	(2 0 0)	5.75	a = 11.52 b = 4.16 c = 4.43 [19]
	25.3	(2 0 1)	3.51	
	27.14	(1 1 1)	3.28	
	31.06	(4 0 0)	2.87	
	47.4	(6 0 0)	1.9	
	49.6	(5 1 1)	1.8	
	51.9	(4 0 2)	1.75	
	57.7	(5 0 2)	1.59	
	60.26	(2 0 2)	1.5	
	64.86	(8 0 0)	1.4	
	67.9	(3 0 3)	1.3	
	84.02	(3 2 3)	1.15	

| 10 µm | EHT = 20 kV
WD = 8.5 mm | Signal A = SE1
Photo no. = 740 | Date: 13 Jan 2017
Time: 11:09:50 | ZEISS |
| 10 µm | EHT = 15 kV
WD = 8.5 mm | Signal A = SE1
Photo no. = 2701 | Date: 28 Jan 2017
Time: 14:22:49 | ZEISS |
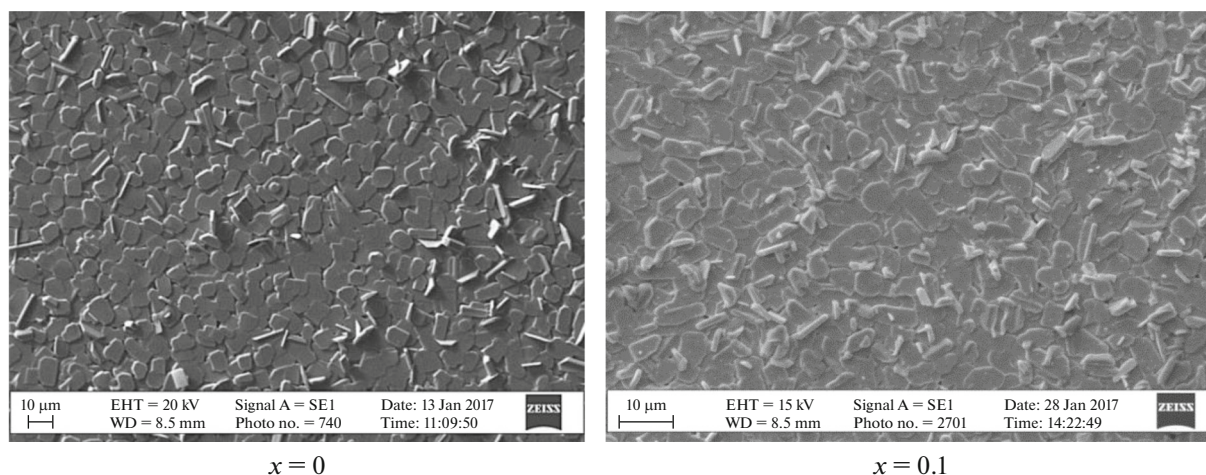
$x = 0$ $x = 0.1$

Fig. 2. SEM images of surface of $(ZnSe)_x(SnSe)_{1-x}$ films having composition with $x = 0$ and $x = 0.1$.

Table 3. Electrical parameters of $(ZnSe)_x(SnSe)_{1-x}$ films

$(ZnSe)_x(SnSe)_{1-x}$	$x = 0$	$x = 0.1$
Conductivity type	p	p
Electrical conductivity σ, $(\Omega\,cm)^{-1}$ at 300 K	15	0.16
Specific resistance ρ, Ω cm at 300 K	6×10^{-2}	6.2
Substrate temperature T_s, °C	500	500

bandgap component is determined by the decrease in the concentration of free carriers.

CONCLUSIONS

The morphological, structural, and electrical properties of $(ZnSe)_{0.1}(SnSe)_{0.9}$ films produced at a substrate temperature of 500°C have been studied.

The results of SEM and XRD analysis data show that the films have an orthorhombic polycrystalline structure; the sizes of film grains is 5−6 µm.

The results from measuring the electrical properties of the films show that the electrical conductivity of the films with a molar content of ZnSe $x = 0.1$ decreased compared to SnSe, and the films have p-type conductivity.

ACKNOWLEDGMENTS

REFERENCES

1. http://www.pv-magazine.com/news/details/beitrag/first-solar-sets-new-cadmium-telluride-thin-film-cell-efficiency-record-at-2.1_100023341/#ixzz415kIS7YW.

2. http://www.businesswire.com/news/home/2013040-9006059/en/Solar-Sets-CdTe-Module-Efficiency-World-Record.

3. Philip, J., Roland, W., Dimitrios, H., et al., *Phys. Status Solidi RRL,* 2016, vol. 10, no. 8, pp. 583−586.

4. Takuya, K. and Solar, F., in *Proceedings of the 7th International Workshop on CIGS Solar Cell Technology IW-CIGSTech 7, June 20−24, 2016, Munich, Germany.*

5. Wei, W., Winkler, M.T., et al., *Energy Mater.,* 2013.

6. Todorov, T.K. and Jiang, T., *Adv. Energy Mater.,* 2013, vol. 3, pp. 34−38.

7. Kumar, V., Anita, S., et al., *Infrared Phys. Technol.,* 2015, vol. 69, pp. 222−227.

8. Zhiqiang, L., Xu, C., Hongbing, Z., et al., *Sol. Energy Mater. Sol. Cells,* 2017, vol. 161, pp. 190−196.

9. Koji, T., Tsuyoshi, M., and Takahiro, W., *Thin Solid Films,* 2015, vol. 582, pp. 263−268.

10. Vasudeva, R., Minnam, R., Sreedevi, G., et al., *J. Mater. Sci.: Mater. Electron.,* 2016, vol. 27, pp. 5491−5508.

11. Chen, C., Wang, L., Gao, L., et al., *ACS Energy Lett.,* 2017, vol. 2, pp. 2125−2132.

12. Jianmin, L., Cong, X., Yaguang, W., et al., *Sol. Energy Mater. Sol. Cells,* 2016, vol. 144, pp. 281−288.

13. Mitsutaro, U., Yasuhiko, T., Shin, T., et al., *J. Appl. Phys.,* 2015, vol. 118, p. 154.

14. Shallal, I.H., *J. Chem., Biol. Phys. Sci., Sect. C,* 2015, vol. 5, no. 3, p. 2760−2768.

15. Madelung, O., Rössler, U., and Schulz, M., *Semimagnetic Compounds,* Berlin, Heidelberg: Springer, 1999, vol. 41, pp. 1−24.

16. Green, M.A., Hishikawa, Y., and Warta, W., *Prog. Photovolt. Res. Appl.,* 2017, no. 25, pp. 668−676.

17. NREL 2017. www.nrel.gov/pv/assets/images/efficiency-chart.png.

18. Kouchkarov, K.M., Razykov, T.M., Ferekides, Ch., et al., *Appl. Sol. Energy,* 2015, vol. 51, no. 4, pp. 314−318.

19. Razykov, T.M., Kuchkarov, K.M., and Ergashev, B.A., *Geliotekhnika,* 2017, no. 2, pp. 3−8.

20. Razykov, T.M., Shukurov, A.X., and Atabayev, O.K., *Geliotekhnika,* 2017, no. 3, pp. 7−11.

21. Razykov, T.M., *Geliotekhnika,* 1988, no. 4, pp. 3−6.

22. Razykov, T.M., *Appl. Surf. Sci.,* 1991, vols. 48−49, no. 1, pp. 89−92.

Translated by Yu. Bezlepkina